

Research Article

Amphiphilic Ruthenium(II) Terpyridine Sensitizers with Long Alkyl Chain Substituted β -Diketonato Ligands: An Efficient Coadsorbent-Free Dye-Sensitized Solar Cells

Ashraful Islam,^{1,2} Surya Prakash Singh,¹ Masatoshi Yanagida,¹
Mohammad Rezaul Karim,² and Liyuan Han¹

¹ International Center for Materials Nanoarchitectonics (MANA) and Advanced Photovoltaics Center,
National Institute for Materials Science (NIMS), 1-2-1 Sengen, Tsukuba, Ibaraki 305-0047, Japan

² Center of Excellence for Research in Engineering Materials (CEREM), College of Engineering, King Saud University,
Riyadh 11421, Saudi Arabia

Correspondence should be addressed to Ashraful Islam, islam.ashraful@nims.go.jp

Received 16 October 2010; Accepted 3 December 2010

Academic Editor: Mohamed Sabry Abdel-Mottaleb

Copyright © 2011 Ashraful Islam et al. This is an open access article distributed under the Creative Commons Attribution License, which permits unrestricted use, distribution, and reproduction in any medium, provided the original work is properly cited.

Three alkyl-substituted β -diketonato-ruthenium(II)-polypyridyl sensitizers with different alkyl chain lengths, [Ru(tctpy)(tfpd)(NCS)] (**A1**), [Ru(tctpy)(tfdd)(NCS)] (**A2**), and [Ru(tctpy)(tfid)(NCS)] (**A3**), were designed and synthesized for dye-sensitized solar cells (DSCs) to investigate the effect of bulky alkyl chain substituents on the photovoltaic performances (where tctpy = 4,4',4''-tricarboxy-2,2':6',2''-terpyridine, tfpd = 1,1,1-trifluoropentane-2,4-dione, tfdd = 1,1,1-trifluorodecane-2,4-dione, and tfid = 1,1,1-trifluoroicosane-2,4-dione). These complexes exhibit a broad metal-to-ligand charge transfer absorption band over the whole visible range extending up to 950 nm. All complexes were examined in the presence and absence of the coadsorbent deoxycholic acid (DCA) in dye-bath solutions. These sensitizers, when anchored to nanocrystalline TiO₂ films, achieve efficient sensitization to TiO₂ electrodes. Under standard AM 1.5 sunlight, the complex **A3** containing long alkyl chain length of C₁₆ yielded a short-circuit photocurrent density of 18.0 mA/cm², an open-circuit voltage of 0.64 V, and a fill factor of 0.66, corresponding to an overall conversion efficiency of 7.6% in the absence of DCA. The power conversion efficiency of **A1** sensitized DSCs was significantly increased upon the addition of DCA as compared to that in the absence of DCA. However, the photovoltaic performance of **A3** was not dependent on DCA at all, probably due to the inherent structural nature of the **A3** molecule.

1. Introduction

In general, dye-sensitized solar cells (DSCs) comprise a nanocrystalline titanium dioxide (TiO₂) electrode modified with a dye and fabricated on a transparent conducting oxide TCO, a platinum counter electrode, and an electrolyte solution with a dissolved iodide ion/triiodide (I⁻/I₃⁻) redox couple between the electrodes [1–5]. Among these elements, the photosensitizer plays a vital role for the light harvesting efficiency. Many sensitizers, including organic sensitizers [6] and transition metal complexes [7–16], have been employed in DSCs. Ru(II) polypyridyl sensitized nanocrystalline TiO₂ solar cells yielding solar to electric power conversion efficiency of over 11% under standard AM 1.5 condition [13, 14]. This is because of their intense

charge-transfer (CT) absorption in the whole visible range, and the absorption properties can be tuned by changing the donor-acceptor properties of the ligand in a controlled manner. Photoexcitation of the charge-transfer (CT) excited states of the adsorbed dye leads to an efficient injection of electrons into the conduction band of the TiO₂.

Ru(II) 4,4',4''-tricarboxy-2,2':6',2''-terpyridine based dyes show efficient panchromatic sensitization of nanocrystalline TiO₂ solar cell that make these class of sensitizers as potential candidates for near-IR dye development [7, 9, 13, 15, 16]. We have reported a series of Ru(II) 4,4',4''-tricarboxy-2,2':6',2''-terpyridine based dye containing β -diketonato ligand that efficiently sensitized nanocrystalline TiO₂ over the whole visible range extending into the near IR region [10, 12, 15, 16]. An important feature of

β -diketonato ligand is its structural versatility due to presence of three substituents on the ligand. Therefore, a desired electronic environment on the metal center, improvement of light harvesting efficiency by extending π -conjugated system, and also introduction of bulky substituent to suppress dye aggregation on TiO_2 surface is possible by molecular designing of the three substituents on the β -diketonato ligand.

Coadsorbents are usually added in the dye solutions to suppress aggregate formation resulting in an improved performance of DSCs through increasing both the short-circuit photocurrent density (J_{sc}) and the open-circuit voltage (V_{oc}) [10, 12, 13, 15–23]. Such aggregate formation has been suggested to promote unwanted intermolecular energy transfer or nonradiative decay pathways, thus reducing the electron injection efficiency. Organic dyes have been found to be more susceptible to aggregate formation compared to Ru-polypyridine based dye [19–23]. Conversely, Ru-bipyridyl based dye has been shown not to form aggregates and addition of coadsorbent in dye-bath solutions only yields a modest or no increase in photocurrents [8, 14]. Although Ru(II) 4,4',4''-tricarboxy-2,2':6',2''-terpyridine based panchromatic sensitizers containing NCS and/or β -diketonato ligand show potential candidates for further improvement of device efficiency, they are susceptible to aggregate formation resulting in a poor device performance without additive in dye-bath solutions [7, 9–13, 15, 16]. In addition, some works showed that the power conversion efficiency of DSCs can be further improved by introducing bulky alkyl chains into the dye structure to obtain an insulating effect of dye layer on the TiO_2 surface [19, 24–27]. Considering the high potentiality of efficient DSCs based on Ru(II)-terpyridine dyes, a strategic structural modification of these dyes is an effective approach to improve light harvesting efficiency in the near-IR region and also suppression of aggregate formation resulting in a coadsorbent-free efficient device processing. Recently we have reported that a β -diketonato ruthenium(II)-tricarboxy-2,2':6',2''-terpyridine sensitizer with extended π -conjugated system by introducing a triphenylamine substituted β -diketonato ligand shows efficient sensitization of nanocrystalline TiO_2 over the whole visible range extending up to 1000 nm [16]. Here we report the synthesis and characterization of terpyridine-ruthenium(II) complexes with β -diketonato ligands having different substituted alkyl chain lengths 1,1,1-trifluoropentane-2,4-dione (tfpd), 1,1,1-trifluorodecane-2,4-dione (tfdd), and 1,1,1-trifluoroicosane-2,4-dione (tfid) and investigated their effects on DSCs performance in the presence and absence of deoxycholic acid (DCA) as a coadsorbent, with the aid of photophysical, and photoelectrochemical measurements. The molecular structures of the complexes $[\text{Ru}(\text{tctpy})(\text{tfpd})(\text{NCS})]$ (**A1**), $[\text{Ru}(\text{tctpy})(\text{tfdd})(\text{NCS})]$ (**A2**), and $[\text{Ru}(\text{tctpy})(\text{tfid})(\text{NCS})]$ (**A3**), and DCA are shown in Figure 1.

2. Experimental Details

2.1. Materials. The following chemicals were purchased and used without further purification: hydrated ruthenium trichloride (from Aldrich), ammonium thiocyanate

(from TCI), 1,1,1-trifluoropentane-2,4-dione (tfpd) (from Aldrich), and LH-20 Sephadex gel (from Sigma). 1,1,1-trifluorodecane-2,4-dione (tfdd) [28], 1,1,1-trifluoroicosane-2,4-dione (tfid) [28] and $\text{Ru}(\text{H}_3\text{tctpy})\text{Cl}_3$ [11] were synthesized using the literature procedures. Complexes $[\text{Ru}(\text{tctpy})(\text{tfpd})(\text{NCS})]$ (**A1**) and $[\text{Ru}(\text{tctpy})(\text{tfid})(\text{NCS})]$ (**A3**) were prepared using the literature procedure [15].

Synthesis of $[\text{Ru}(\text{tctpy})(\text{tfdd})(\text{NCS})]$ (A2**).** Using the same conditions as for complex **A1**, and starting from ligand 1,1,1-trifluorodecane-2,4-dione (tfdd), the title compound was obtained as a dark green powder, $[\text{Ru}(\text{tctpy})(\text{tfdd})(\text{NCS})]$ (**A2**). Yield was 60%; MS (ESIMS): m/z : 249.3 ($\text{M}-3\text{H}$) $^{3-}$, 374.5 ($\text{M}-2\text{H}$) $^{2-}$. ^1H NMR (300 MHz, D_2O -NaOD): δ 8.76 (2H, s), 8.72 (2H, d), 8.52 (H, d), 8.46 (H, d), 7.85 (H, d), 7.78 (H, d), 5.84 (0.5H, s), 5.82 (0.5H, s), 2.53 (2H, m), 1.55–0.80 (8H, m), 0.50 (3H, m), Anal. Calcd for $\text{C}_{29}\text{H}_{28}\text{F}_3\text{N}_4\text{O}_8\text{RuS}\cdot(\text{H}_2\text{O})_2$: C, 44.27; H, 4.10; N, 7.12, found: C, 45.01; H, 4.21; N, 6.88.

2.2. Analytical Measurements. UV-visible spectra were recorded on a Shimadzu UV-3101PC spectrophotometer. Steady-state emission spectra were recorded using a grating monochromator (Triax 1900) with a CCD image sensor. The redox potential of the complexes was measured using a standard three-electrode apparatus.

2.3. Preparation of TiO_2 Electrode and Dye-Loading Measurements. Nanocrystalline TiO_2 photoelectrodes of about 20 μm thickness (area: 0.25 cm^2) were prepared using a variation of a method reported by Nazeeruddin et al. for solar cells measurements [11]. We also prepared transparent TiO_2 film of 7 μm thicknesses to check the adsorption properties of the complexes on to TiO_2 film using the same method. The dye-loading measurement on TiO_2 films was carried out by desorbing the dye into 0.1 M NaOH, solution in CH_3OH and the dye load on the TiO_2 film was estimated by means of an ultraviolet-visible absorption spectroscopy.

2.4. Fabrication of Dye-Sensitized Solar Cell. Two-electrode sandwich cell configurations were used for photovoltaic measurements. The dye-deposited TiO_2 film was used as the working electrode and a platinum-coated conducting glass as the counter electrode. The two electrodes were separated by a surlyn spacer (40 μm thick) and sealed up by heating the polymer frame. The electrolyte was composed of 0.6 M dimethylpropyl-imidazolium iodide (DMPII), 0.05 M I_2 , and 0.1 M LiI in acetonitrile (AN).

3. Results and Discussion

3.1. Photophysical Properties. The absorption, emission, and electrochemical properties of complexes **A1**, **A2**, and **A3** are summarized in Table 1. All the complexes show similar absorption spectra in ethanol-methanol solution as shown in Figure 2. The bands in the visible region are assigned to metal-to-ligand charge-transfer (MLCT) transitions and in the UV region to ligand π - π^* transitions

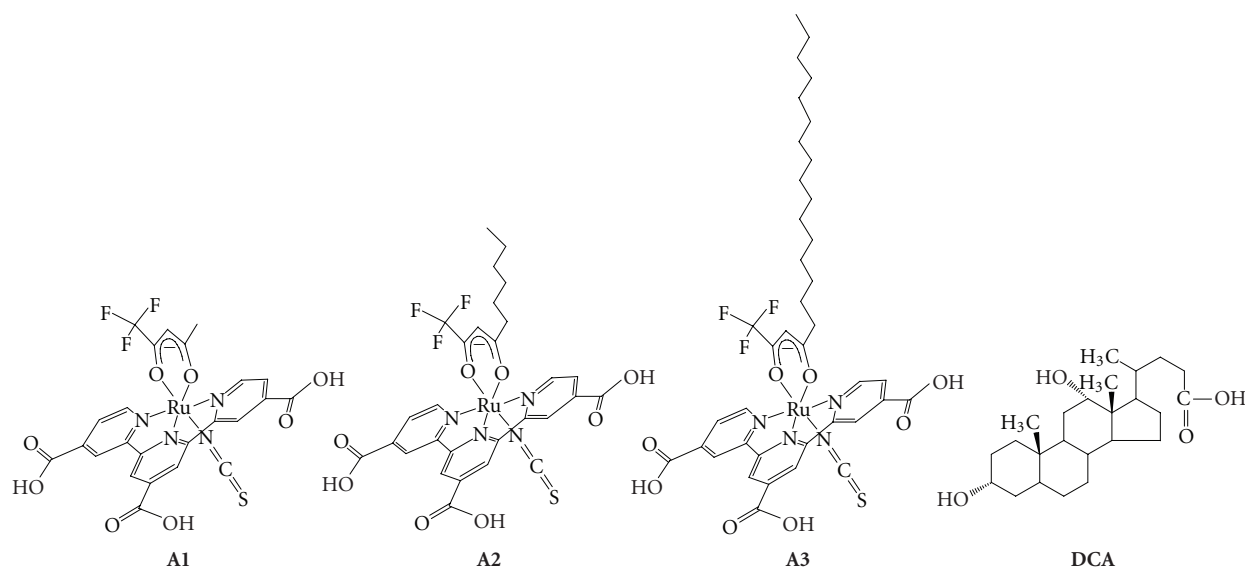
FIGURE 1: Molecular structures of complexes **A1**, **A2**, **A3**, and **DCA**.

TABLE 1: Absorption, luminescence, and electrochemical properties of the ruthenium complexes.

Sensitizer	Absorption, $^a\lambda_{\text{max}}/\text{nm}$ ($\epsilon/10^3 \text{ M}^{-1} \text{ cm}^{-1}$)	Emission $\lambda_{\text{max}}^b/\text{nm}$		Emission τ^b/ns		$E(\text{Ru}^{3+/2+})^c$ / versus SCE	$E^*(\text{Ru}^{3+/2+})^d$ / versus SCE
		298 K	77 K	298 K	77 K		
A1	280 (27.6), 331 (22.7), 422 (14.7), 606 (7.0)	940	905	16	160	+0.68	−0.90
A2	280 (28.2), 331 (23.1), 418 (13.6), 605 (7.1)	945	900	15	214	+0.70	−0.95
A3	280 (30.0), 331 (23.6), 422 (14.7), 606 (7.0)	950	910	16	152	+0.70	−0.95

^a Measured in 4 : 1 v/v ethanol : methanol at room temperature.

^b The emission spectra and emission lifetime were obtained by exciting into the lowest MLCT band in 4 : 1 v/v ethanol : methanol.

^c Half-wave potentials assigned to the $\text{Ru}^{3+/2+}$ couple for ruthenium sensitizers bound to nanocrystalline TiO_2 film, measured in 0.1 M LiClO_4 acetonitrile solution.

^d Calculated from $E^*(\text{Ru}^{3+/2+}) = E(\text{Ru}^{3+/2+}) - E^{0-0}$; E^{0-0} values were estimated from the 5% intensity level of the emission spectra at 77 K.

of 4,4',4''-tricarboxy-2,2':6',2''-terpyridine [29]. The low-energy MLCT band maximum of complex **A1** is observed at 606 nm with the molar extinction coefficient of about $7000 \text{ M}^{-1} \text{ cm}^{-1}$. The emission spectra of complex **A3** in ethanol-methanol mixed solvents at 77 and 298 K are presented in Figure 3. The luminescence data are displayed in Table 1. At 77 K, complexes **A1**, **A2**, and **A3** displayed excited-state lifetimes ranging from 152 to 214 ns. The lifetimes decreased significantly with increasing temperature, to 15–16 ns in fluid solution at 298 K. The very short-lived excited state in fluid solution may be caused by efficient nonradiative decay via low-lying ligand-field excited states [30]. The excited-state lifetime of all the complexes is long enough for the process of electron injection into the conduction band of the TiO_2 electrode to be efficient [31]. To be a suitable sensitizer in DSCs, the band structure of the metal complex should match the energy level of the semiconductor anode and the redox electrolyte or the hole conductor. The electrochemical data of the complexes measured in methanol solution are summarized in Table 1. All the complexes exhibit quasireversible oxidation wave for the $\text{Ru}^{3+/2+}$ couple ranging from +0.68 to +0.70 V versus SCE. The formation of an

MLCT excited state of these complexes formally involves the oxidation of a HOMO having metal t_{2g} orbital character and reduction of a terpyridine-based LUMO.

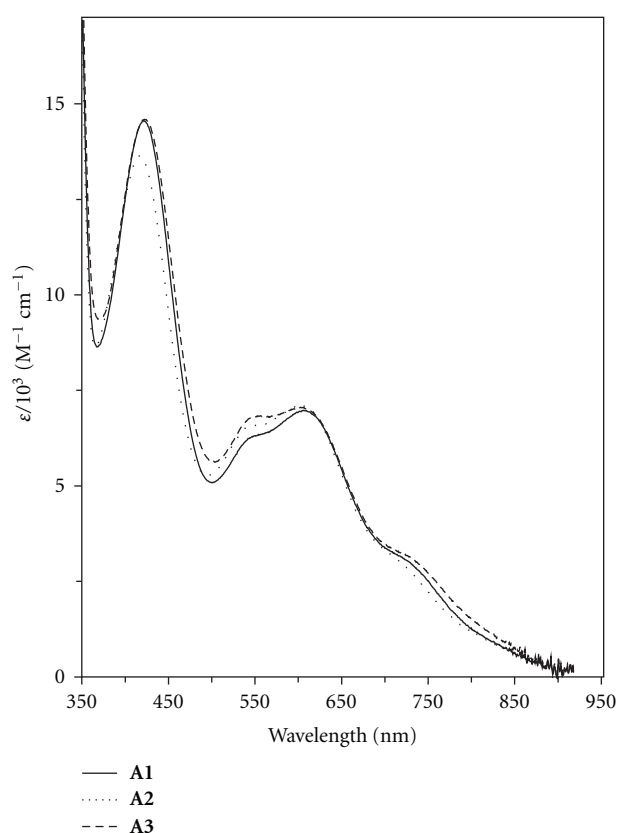
3.2. Dye Adsorption Behavior. Figure 4 shows the absorption spectra of complexes **A1**, **A2**, and **A3** adsorbed onto a nanocrystalline $7 \mu\text{m}$ thick TiO_2 film. All the complexes show almost similar absorption spectra on TiO_2 film but the absorbance decreases with increasing alkyl chain length of the substituted β -diketonato ligands. We compare the UV-vis absorption spectra for the **A1** dye-loaded TiO_2 films, with and without the addition of DCA during the dye-loading process. When DCA was added in the dye solution, the dye-sensitized TiO_2 film cogenerated along with DCA and showed a similar absorption spectrum. The absorbance at around 570 nm decreased by 18% compared with that of without DCA. The competition of DCA with the dye for binding to the TiO_2 surface is responsible for the decrease in dye adsorption. The adsorbed amount of dye on the TiO_2 film with and without DCA was listed in Table 2. It was noticed that the amount of dye adsorbed onto the TiO_2 surface was

TABLE 2: Adsorbed amount of dye and cell performance^a of **A1**, **A2**, and **A3** sensitizers with and without DCA.

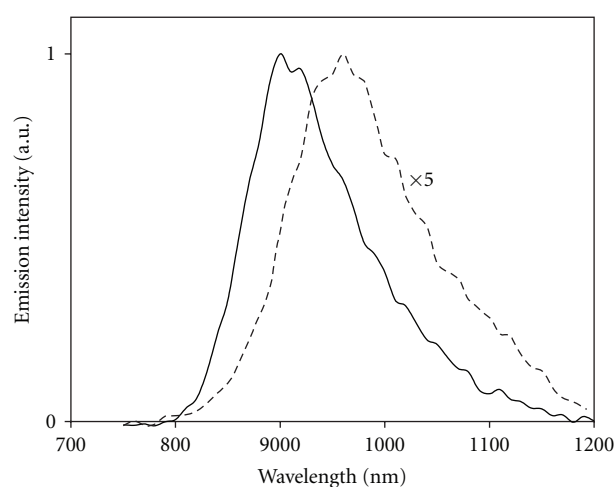
Sensitizer	DCA (mM)	IPCE _{max}	J_{sc} (mA cm ⁻²)	V_{oc} (V)	FF	η (%)	Dye load ^b (10 ⁻⁸ mol cm ⁻²)
A1	0	67	15.9	0.53	0.63	5.31	11.5
	15	74	18.5	0.56	0.64	6.63	7.6
A2	0	69	17.2	0.57	0.63	6.18	9.4
	15	72	18.1	0.58	0.65	6.82	7.2
A3	0	72	18.0	0.64	0.66	7.60	7.3
	15	70	17.4	0.64	0.67	7.46	6.6

^a Conditions: sealed cells; coadsorbate, DCA 0 or 15 mM; photoelectrode, TiO₂ (20 μm thickness and 0.25 cm²); electrolyte, 0.6 M DMPII, 0.1 M LiI, 0.05 I₂ in AN; irradiated light, AM 1.5 solar light (100 mW cm⁻²). J_{sc} : short-circuit photocurrent density; V_{oc} : open-circuit photovoltage; FF: fill factor; η : total power conversion efficiency; IPCE: incident photon-to-current conversion efficiency.

^b Surface concentration of the dye molecules on TiO₂ film.

FIGURE 2: UV-vis absorption spectra of complexes **A1**, **A2**, and **A3** in ethanol-methanol (4 : 1) solution.

reduced in the presence of DCA, as compared to that without DCA in the dye bath. For complex **A1**, the difference between the amount of dye adsorbed onto the TiO₂ surface in the presence and absence of DCA in the dye bath is 34%. This is maybe due to the suppression of dye aggregation in the presence of DCA. For complex **A3**, having long alkyl chain length, the amount of dye adsorbed onto the TiO₂ surface in the absence of DCA decreases compared to that of **A1**. There was a small decrease in dye load when DCA was added into the dye bath. The amount of complex **A3** adsorbed onto the TiO₂ surface decreased by only 9% in the presence of DCA,

FIGURE 3: Emission spectra of complex **A3** in ethanol-methanol (4 : 1) solution at 77 K (—) and 298 K (---).

whereas the complex **A1** load was reduced about 34%. The long alkyl chain present on complex **A3**, may be suppress the aggregate formation onto the TiO₂ surface and works like DCA. It is suggested that **A3** form an ordered dye layer on TiO₂ surface and binds more strongly to the TiO₂ surface than DCA.

3.3. Photovoltaic Properties. The photovoltaic performance of complexes **A1**, **A2**, and **A3** on nanocrystalline TiO₂ electrode was studied under standard AM 1.5 irradiation (100 mW cm⁻²) using an electrolyte with a composition of 0.6 M dimethylpropyl-imidazolium iodide (DMPII), 0.05 M I₂, and 0.1 M LiI in acetonitrile in the presence and absence of DCA in the dye bath. The short-circuit photocurrent density (J_{sc}), open-circuit voltage (V_{oc}), fill factors (FF), and overall cell efficiencies (η) for each dye-TiO₂ electrode are summarized in Table 2. Figure 5 shows the photocurrent action spectra for complexes **A1** and **A3** in the presence and absence of DCA, where the incident photon to current conversion efficiency (IPCE) values is plotted as a function of wavelength. All complexes achieved efficient sensitization of nanocrystalline TiO₂ over the whole visible

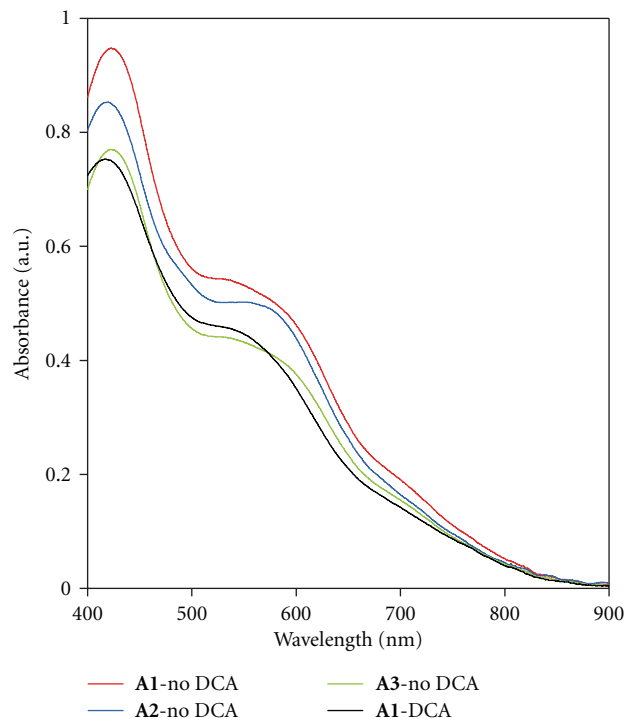


FIGURE 4: Absorption spectra of complexes **A1**, **A2**, and **A3** adsorbed onto a nanocrystalline 7 μm thick TiO_2 film.

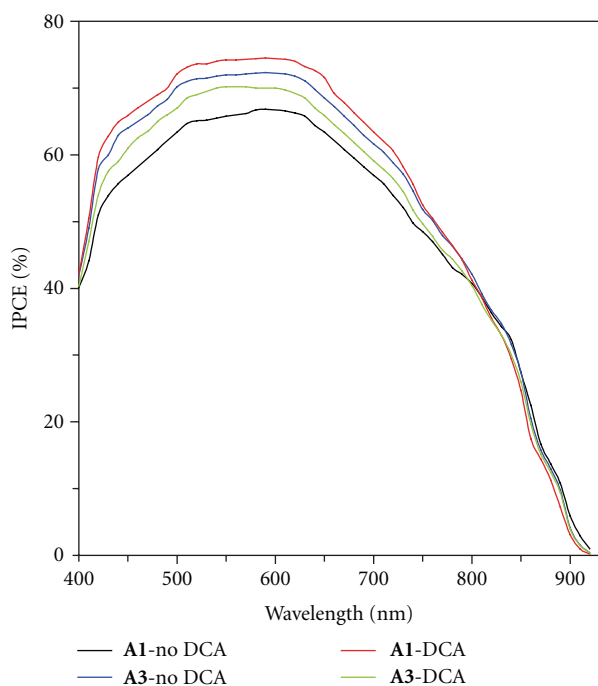


FIGURE 5: Photocurrent action spectra obtained with complexes **A1** and **A3** with and without **DCA** addition during the sensitization process. Incident photon-to-current conversion efficiency is plotted as a function of wavelength. A sandwich type sealed cell configuration was used to measure this spectrum. The electrolyte composition was 0.6 M DMPII, 0.05 M I_2 , and 0.1 M LiI in acetonitrile.

range extending into the near IR region. The maximum IPCE values of complexes **A1–A3** are given in Table 2.

As shown in Table 2, a solar cell containing complex **A1** yielded a short-circuit photocurrent density (J_{sc}) of 15.9 mA cm^{-2} , an open-circuit photovoltage (V_{oc}) of 0.53 V, and a fill factor (FF) of 0.63, corresponding to an overall conversion efficiency (η) of 5.3% in the absence of DCA. The addition of DCA gave a pronounced efficiency enhancement up to 6.6% with a short-circuit photocurrent density of 18.5 mA cm^{-2} and an open-circuit photovoltage of 0.56 V. Although the amount of complex **A1** adsorbed on the TiO_2 film decreased to 34% with the addition of DCA during the dye-loading process, the values of J_{sc} , V_{oc} , and, thus, the efficiency were increased as compared to the case without DCA addition. As shown in Figure 5, complex **A1** shows the IPCE value of 67% in the plateau region in the absence of DCA, and the maximum IPCE value increased up to 74% with the addition of DCA during the dye-loading process. The observed changes in J_{sc} agreed well with the corresponding IPCE spectra for **A1**-sensitized DSCs with and without the addition of DCA. The main possible explanation is that the coadsorption of DCA prevents dye aggregation, which can cause intermolecular energy transfer and sequentially result in the excited-state quenching of the dyes [19]. As a result, the reduction of dye load on the TiO_2 surface in the presence of DCA consequently results in more efficient electron injection from the excited dyes to the TiO_2 conduction band [19]. A more efficient electron injection thus compensates for the less amount of dye adsorption.

It is interesting to find that **A3**-sensitized DSCs having a long alkyl chain, in the absence of DCA, give a high overall conversion efficiency of 7.6% with a short-circuit photocurrent density of 18.0 mA cm^{-2} and an open-circuit photovoltage of 0.64 V. The photovoltaic performance of **A3**-sensitized DSCs is higher than that of **A3**-sensitized DSCs with the addition of DCA during the dye-loading process. This indicates that the photovoltaic performance of bulky alkyl chain substituted sensitizer **A3** was not dependent on additive DCA. It is expected that the injection of electron into the TiO_2 conduction band and the recombination of electrons in the TiO_2 film with the oxidized species in the redox electrolyte is unaffected in **A3**-sensitized DSCs with and without DCA addition. As shown in Table 2, the amount of adsorbed **A3** on TiO_2 surface with and without DCA addition is almost the same and also shows similar photovoltaic performance which suggest a self-assembly property of complex **A3** due to the presence of a bulky alkyl chain substitute in the structure. A self-assembly property of the dye during the sensitization of TiO_2 film is important to obtain efficient surface coverage and efficient electron injection and thus obtain high photovoltaic performance of DSCs [19]. Figure 1 showed that the **A3** sensitizer contains long alkyl chain in the β -diketonato ligand which may produce surface blocking through steric hindrance, preventing the access of electrons to the redox electrolyte, which will be in favor of higher V_{oc} . On the other hand, this bulky alkyl group may not only facilitate the ordered molecular arrangement on the TiO_2 surface but also keep dye molecules at a distance, which may suppress

possibly intermolecular dye interaction, favoring higher J_{sc} [19]. The protection by the alkyl chain is proven to be more efficient as compared to the coadsorption of DCA under the examined conditions. However, the less efficient surface protection in **A1** sensitizer resulted in poor photovoltaic performance. In conclusion, higher power conversion efficiencies were obtained for DSCs based on **A3** with bulky alkyl substituent due to the inherent properties of the dye molecule.

As illustrated in Figure 1, **A2** sensitizer has an alkyl chain length of C_6 on the β -diketonato ligand which is shorter than **A3** sensitizer (C_{16}). Thus, an expected intermediate performance for **A2**-sensitized DSCs was obtained in comparison with **A1** and **A3** under both conditions, with and without the DCA addition. From Table 2, it is clear that the dye load of **A2** dropped by about 23% due to the addition of DCA in the dye bath. However, the value of J_{sc} increased with decreasing dye coverage, probably due to the same reason as mentioned for **A1**.

The **A3** sensitizer having long alkyl chain substituent on the β -diketonato ligand shows the best performance in this series. Thus, this class of diketonato ruthenium complexes serves as a basis for further design of new potential sensitizers by introducing suitable substituents on the diketonato ligand to prevent surface aggregation of the sensitizer for efficient injection efficiencies and furthermore to enhance the molar extinction coefficient of the sensitizer.

4. Conclusions

Three panchromatic photosensitizers **A1**, **A2**, and **A3** based on 4,4',4''-tricarboxy-2,2':6',2''-terpyridine-ruthenium(II) complexes with one β -diketonato chelating ligand containing different bulky alkyl chain lengths between C_1 – C_{16} were developed and systematically characterized using electrochemical and spectroscopic methods. The complexes achieved efficient sensitization of nanocrystalline TiO_2 over the whole visible range extending into the near IR region (ca. 950 nm). These dyes showed gradually enhanced photovoltaic performance with increasing the alkyl chain length. The photovoltaic data of these new complexes show 7.6% power conversion efficiency under standard AM 1.5 irradiation (100 mW cm^{-2}). To understand the effect of the bulky substituent on the photovoltaic performance of DSCs, we investigated the photovoltaic performances of **A1**-, **A2**-, and **A3**-sensitized DSCs with and without DCA addition in the dye bath. We notice that the photovoltaic performance of **A3**-sensitized DSCs containing bulky alkyl chain length of C_{16} was independent of the DCA, while the **A2** bearing alkyl chains length of C_6 and **A1** without alkyl chain showed 10% and 24%, respectively, improvement in photovoltaic performance in the presence of the DCA. Without DCA, **A3**-based DSCs were still superior to both **A1** and **A2** in the presence of DCA. This is probably due to the inherently structural nature of **A3** molecule, functionalized with bulky alkyl chain substituent, which resulted in excellent photovoltaic performance.

References

- [1] B. O'Regan and M. Grätzel, "A low-cost, high-efficiency solar cell based on dye-sensitized colloidal TiO_2 films," *Nature*, vol. 353, no. 6346, pp. 737–740, 1991.
- [2] A. Hagfeldt and M. Grätzel, "Light-induced redox reactions in nanocrystalline systems," *Chemical Reviews*, vol. 95, no. 1, pp. 49–68, 1995.
- [3] A. Hagfeldt and M. Grätzel, "Molecular photovoltaics," *Accounts of Chemical Research*, vol. 33, no. 5, pp. 269–277, 2000.
- [4] M. Grätzel, "Solar energy conversion by dye-sensitized photovoltaic cells," *Inorganic Chemistry*, vol. 44, no. 20, pp. 6841–6851, 2005.
- [5] M. Grätzel, "Conversion of sunlight to electric power by nanocrystalline dye-sensitized solar cells," *Journal of Photochemistry and Photobiology A*, vol. 164, no. 1–3, pp. 3–14, 2004.
- [6] A. Mishra, M. K. R. Fischer, and P. Buerle, "Metal-Free organic dyes for dye-sensitized solar cells: from structure: property relationships to design rules," *Angewandte Chemie*, vol. 48, no. 14, pp. 2474–2499, 2009.
- [7] A. Islam, H. Sugihara, and H. Arakawa, "Molecular design of ruthenium(II) polypyridyl photosensitizers for efficient nanocrystalline TiO_2 solar cells," *Journal of Photochemistry and Photobiology A*, vol. 158, no. 2–3, pp. 131–138, 2003.
- [8] A. Hagfeldt, G. Boschloo, L. Sun, L. Kloo, and H. Pettersson, "Dye-sensitized solar cells," *Chemical Reviews*, vol. 110, no. 11, pp. 6595–6663, 2010.
- [9] T. Funaki, M. Yanagida, N. Onozawa-Komatsuzaki, K. Kasuga, Y. Kawanishi, and H. Sugihara, "Efficient panchromatic sensitization of nanocrystalline TiO_2 -based solar cells using 2-pyridinecarboxylate-substituted Ruthenium(II) complexes," *Chemistry Letters*, vol. 38, no. 1, pp. 62–63, 2009.
- [10] A. Islam, F. A. Chowdhury, Y. Chiba et al., "Synthesis and characterization of new efficient tricarboxyterpyridyl (β -diketonato) ruthenium(II) sensitizers and their applications in dye-sensitized solar cells," *Chemistry of Materials*, vol. 18, no. 22, pp. 5178–5185, 2006.
- [11] M. K. Nazeeruddin, P. Péchy, T. Renouard et al., "Engineering of efficient panchromatic sensitizers for nanocrystalline TiO_2 -based solar cells," *Journal of the American Chemical Society*, vol. 123, no. 8, pp. 1613–1624, 2001.
- [12] A. Islam, F. A. Chowdhury, Y. Chiba et al., "Ruthenium(II) tricarboxyterpyridyl complex with a fluorine-substituted β -diketonato ligand for highly efficient dye-sensitized solar cells," *Chemistry Letters*, vol. 34, no. 3, pp. 344–345, 2005.
- [13] Y. Chiba, A. Islam, Y. Watanabe, R. Komiya, N. Koide, and L. Han, "Dye-sensitized solar cells with conversion efficiency of 11.1%," *Japanese Journal of Applied Physics, Part 2*, vol. 45, no. 24–28, pp. L638–L640, 2006.
- [14] Q. Wang, S. Ito, M. Grätzel et al., "Characteristics of high efficiency dye-sensitized solar cells," *Journal of Physical Chemistry B*, vol. 110, no. 50, pp. 25210–25221, 2006.
- [15] A. Islam, H. Sugihara, M. Yanagida et al., "Efficient panchromatic sensitization of nanocrystalline TiO_2 films by β -diketonato ruthenium polypyridyl complexes," *New Journal of Chemistry*, vol. 26, no. 8, pp. 966–968, 2002.
- [16] S. Gao, A. Islam, Y. Numata, and L. Han, "A β -diketonato ruthenium(II) complex with high molar extinction coefficient for panchromatic sensitization of nanocrystalline TiO_2 film," *Applied Physics Express*, vol. 3, no. 6, Article ID 062301, 2010.

- [17] A. Morandeira, I. López-Duarte, B. O'Regan et al., "Ru(II)-phthalocyanine sensitized solar cells: the influence of coadsorbents upon interfacial electron transfer kinetics," *Journal of Materials Chemistry*, vol. 19, no. 28, pp. 5016–5026, 2009.
- [18] Z. Zhang, N. Evans, S. M. Zakeeruddin, R. Humphry-Baker, and M. Grätzel, "Effects of ω -guanidinoalkyl acids as coadsorbents in dye-sensitized solar cells," *Journal of Physical Chemistry C*, vol. 111, no. 1, pp. 398–403, 2007.
- [19] X. Jiang, T. Marinado, E. Gabrielsson, D. P. Hagberg, L. Sun, and A. Hagfeldt, "Structural Modification of organic dyes for efficient coadsorbent-free dye-sensitized solar cells," *Journal of Physical Chemistry C*, vol. 114, no. 6, pp. 2799–2805, 2010.
- [20] H. Chen, H. Huang, X. Huang et al., "High molar extinction coefficient branchlike organic dyes containing Di(*p*-tolyl)phenylamine donor for dye-sensitized solar cells applications," *Journal of Physical Chemistry C*, vol. 114, no. 7, pp. 3280–3286, 2010.
- [21] X. Ren, Q. Feng, G. Zhou, C. H. Huang, and Z. S. Wang, "Effect of cations in coadsorbate on charge recombination and conduction band edge movement in dye-sensitized solar cells," *Journal of Physical Chemistry C*, vol. 114, no. 15, pp. 7190–7195, 2010.
- [22] T. Marinado, M. Hahlin, X. Jiang et al., "Surface molecular quantification and photoelectrochemical characterization of mixed organic dye and coadsorbent layers on TiO₂ for dye-sensitized solar cells," *Journal of Physical Chemistry C*, vol. 114, no. 27, pp. 11903–11910, 2010.
- [23] J. H. Yum, S. J. Moon, R. Humphry-Baker et al., "Effect of coadsorbent on the photovoltaic performance of squaraine sensitized nanocrystalline solar cells," *Nanotechnology*, vol. 19, no. 42, Article ID 424005, 2008.
- [24] S. Ito, H. Miura, S. Uchida et al., "High-conversion-efficiency organic dye-sensitized solar cells with a novel indoline dye," *Chemical Communications*, no. 41, pp. 5194–5196, 2008.
- [25] C. Kim, H. Choi, S. Kim et al., "Molecular engineering of organic sensitizers containing *p*-phenylene vinylene unit for dye-sensitized solar cells," *Journal of Organic Chemistry*, vol. 73, no. 18, pp. 7072–7079, 2008.
- [26] H. Choi, S. Kim, S. O. Kang et al., "Stepwise cosensitization of nanocrystalline TiO₂ films utilizing Al₂O₃ layers in dye-sensitized solar cells," *Angewandte Chemie*, vol. 47, no. 43, pp. 8259–8263, 2008.
- [27] N. Koumura, Z. S. Wang, S. Mori, M. Miyashita, E. Suzuki, and K. Hara, "Alkyl-functionalized organic dyes for efficient molecular photovoltaics," *Journal of the American Chemical Society*, vol. 128, no. 44, pp. 14256–14257, 2006.
- [28] J. C. Sloop, C. L. Bumgardner, and W. D. Loehle, "Synthesis of fluorinated heterocycles," *Journal of Fluorine Chemistry*, vol. 118, no. 1-2, pp. 135–147, 2002.
- [29] A. Mamo, A. Juris, G. Calogero, and S. Campagna, "Near-infrared luminescence at room temperature of two new osmium(II) terdentate polypyridine complexes," *Chemical Communications*, no. 10, pp. 1225–1226, 1996.
- [30] A. Islam, N. Ikeda, A. Yoshimura, and T. Ohno, "Nonradiative transition of phosphorescent charge-transfer states of ruthenium(II)-to-2,2'-biquinoline and ruthenium(II)-to-2,2':6',2''-terpyridine in the solid state," *Inorganic Chemistry*, vol. 37, no. 12, pp. 3093–3098, 1998.
- [31] Y. Tachibana, S. A. Haque, I. P. Mercer, J. R. Durrant, and D. R. Klug, "Electron injection and recombination in dye sensitized nanocrystalline titanium dioxide films: a comparison of ruthenium bipyridyl and porphyrin sensitizer dyes," *Journal of Physical Chemistry B*, vol. 104, no. 6, pp. 1198–1205, 2000.

